LIMNOLOGY
and
OCEANOGRAPHY

ASLO

*Limnol. Oceanogr.* 62, 2017, 2243–2259

doi: 10.1002/lno.10564

# Trace metal composition of size-fractionated plankton in the Western Philippine Sea: The impact of anthropogenic aerosol deposition

**Wen-Hsuan Liao,[1,2,3] Shun-Chung Yang,[1] Tung-Yuan Ho [1,2,3,4]***

[1]Research Center for Environmental Changes, Academia Sinica, Taipei, Taiwan
[2]Earth System Science Program, Taiwan International Graduate Program, Academia Sinica, Taipei, Taiwan
[3]College of Earth Science, National Central University, Taoyuan, Taiwan
[4]Institute of Oceanography, National Taiwan University, Taipei, Taiwan

## *Abstract*

The surface water of the Western Philippine Sea (WPS) receives a significant amount of anthropogenic aerosols from East Asia, serving as an ideal location to investigate the impact of anthropogenic aerosol deposition on trace metal composition and cycling in the Northwestern Pacific Ocean (NWPO). As part of the Taiwan GEOTRACES process study, we have collected size-fractionated plankton from surface water to investigate their metal composition in the open ocean. Elemental ratios in plankton, P- and Al-normalized, are used to evaluate the sources of trace metals and the relative contribution of different metal components in plankton assemblages. Most of the trace metal quotas in plankton are one to two orders of magnitude higher than their intracellular plankton quota, indicating that the majority of the metals are most likely to be extracellularly adsorbed or aggregated on plankton. The metal to Al ratios for most of the trace metals in plankton are also one to two orders of magnitude higher than their lithogenic composition, but are relatively close to metal composition in aerosols collected in situ. This supports the notion that particulate trace metals associated with plankton mainly originate from anthropogenic aerosols, not lithogenic particles. Compared to plankton metal quotas obtained in other oceanic regions, trace metal quotas observed in the WPS rank among the highest for Fe, Mn, Zn, and Cu globally. Our study demonstrates that anthropogenic aerosol deposition has significantly elevated trace metal concentrations in the size-fractionated plankton in the surface water of the NWPO relative to the biological requirements.

Particles play essential roles in regulating material cycling for both major and trace elements in the ocean (Goldberg 1954; Redfield 1958; Bishop et al. 1977). The regulation of elemental distribution in marine water columns involves complicated particle transformation processes, including the coupling processes of adsorption and desorption, aggregation and disaggregation, dissolution and precipitation, suspension and sinking, and biological assimilation and microbial remineralization. Trace metal composition in particles may retain useful information to reflect these internal transformation processes in the oceanic water column and external sources of the elements. For example, phytoplankton intracellular metal composition is directly associated with inorganic trace metal concentrations in ambient seawater as well as the competition of other trace metals possessing similar chemical properties through phytoplankton uptake (Sunda 2012). Trace metal composition in plankton may also reflect the sources of trace metals in oceanic surface water (Ho et al. 2007). With increasing understanding of the importance of particles for trace metal cycling, particulate trace metal related studies have been recognized as an important component in GEOTRACES (Henderson and Marchal 2015; Jeandel et al. 2015), an international study of marine biogeochemical cycles of trace elements and their isotopes for global oceans (Anderson and Henderson 2005). For example, recent studies have started evaluating analytical and sampling methods in order to obtain reliable trace metal composition in marine suspended particles (Planquette and Sherrell 2012; Twining et al. 2015*a*). The North Atlantic Ocean GEOTRACES studies show that lithogenic and biogenic particles both can play important roles in regulating particulate metal composition in the water column (Ohnemus and Lam 2015; Twining et al. 2015*b*).

The characterization and quantification of biotic and abiotic trace metal components and composition in plankton

*Correspondence: tyho@gate.sinica.edu.tw

Additional Supporting Information may be found in the online version of this article.

assemblages and suspended particles is essential in understanding the sources and transformation processes of trace metals in the ocean because biotic and abiotic particles have distinct sources and fates in the marine water columns. However, the separation of marine biotic and abiotic particles is operationally challenging. The association and the relative quantitative contribution of abiotic and biotic components in suspended particles in the ocean still remain largely unknown. Although suspended particles in the surface water of the open ocean are mostly composed of various sizes of phytoplankton and zooplankton, intracellular trace metals are not necessarily the dominant trace metal pool in bulk plankton assemblages. Without knowing the trace metal composition of plankton assemblages and their quantitative contribution in suspended particles in the ocean, the relative contributions of biotic and abiotic particles remains uncertain. Trace metal composition in plankton assemblages is thus essential information to study particulate trace metal cycling in the ocean.

To validate intracellular trace metal composition determined from field studies, Ho et al. (2003) carried out a comprehensive laboratory culture experiment to obtain intracellular metal composition in five major eukaryotic phytoplankton phyla using metal concentrations in culture medium simulating the condition of oceanic surface water. Despite large inter-species variations of metal quota observed ($n = 15$), the averaged metal quotas among different phyla were relatively constrained, $P_{1000}$ $Fe_{7.5 \pm 5.3}$ $Mn_{3.8 \pm 2.4}$ $Zn_{0.80 \pm 0.52}$ $Cu_{0.38 \pm 0.35}$ $Co_{0.19 \pm 0.13}$ $Cd_{0.21 \pm 0.22}$. Moreover, many of the metal quotas are comparable to plankton trace metal composition observed in a few reliable field studies, where the contribution of lithogenic particles was known to be minimal (Bruland et al. 1991; Ho et al. 2003). Coupling the value of the field and laboratory studies, Ho (2006) proposed intracellular trace metal quota in plankton to be $P_{1000}$ $Fe_{5.1 \pm 1.6}$ $Mn_{0.68 \pm 0.54}$ $Zn_{2.1 \pm 0.88}$ $Cu_{0.41 \pm 0.16}$ $Ni_{0.70 \pm 0.54}$ $Co_{0.15 \pm 0.06}$ $Cd_{0.42 \pm 0.20}$. It should be noted that bulk plankton intracellular metal quotas should be considered as a range instead of a fixed number because of the variations of intracellular metal quotas observed among different groups of plankton. Despite their variability, intracellular trace metal quotas are useful for modeling trace metal biogeochemistry and cycling in the ocean globally.

In addition to intracellular metal pool in plankton, metal adsorption and particle aggregation can contribute a significant amount of metals to plankton samples (Ho et al. 2007). Abiotic particles, originating from lithogenic, authigenic, and anthropogenic particles, generally possess much higher metal concentrations than intracellular concentrations in plankton. For example, Fe concentrations in lithogenic particles account for about 5% of lithogenic particle by weight (Hu and Gao 2008), which are around two orders of magnitude higher than its intracellular concentrations in dried plankton by weight (Ho 2006). Aeolian deposition is a major process in transporting abiotic material to the surface water of the open ocean. The Northwestern Pacific Ocean (NWPO) is located right next to East Asia and East China, where about 60% of global coal is consumed (http://www.iea.org/statistics). Elevated fine aerosol optical depth observed by moderate-resolution imaging spectroradiometer shows that massive anthropogenic aerosols generated from fossil fuel burning in East Asia are brought to the remote region of the NWPO through northeastern monsoon in late autumn, winter, and spring. Our previous studies in the South China Sea (SCS) indicated that trace metals in size-fractionated plankton originate from aerosol deposition and that most of the metals are mainly extracellularly adsorbed or aggregated (Ho et al. 2007, 2010). Using Fe and Zn as examples, the averaged total Fe/P and Zn/P ratios in phytoplankton larger than 10 $\mu$m and zooplankton are $120 \pm 91$ mmol mol$^{-1}$ P and $5.5 \pm 2.0$ mmol mol$^{-1}$ P, respectively, about one order of magnitude higher than the intracellular ratios proposed (Ho 2006).

The Western Philippine Sea (WPS), located in the western boundary of the NWPO, also receives a tremendous amount of anthropogenic aerosol deposition and serves as an ideal location to investigate the impact of anthropogenic aerosol deposition on trace metal composition in plankton assemblages of the NWPO (Lin et al. 2015). Taking advantage of the Taiwan GEOTRACES process study carried out in 2013 and 2014, we have collected size-fractionated plankton in the WPS to study the impact of anthropogenic aerosol deposition on trace metal composition in plankton assemblages of the oceanic region.

## Materials

### Sampling

Size-fractionated plankton samples were collected on three cruises carried out in the WPS. Two Taiwan GEOTRACES process study cruises were carried out in July 2013 and March 2014 at eight stations along 23.5°N transect by using R/V Ocean Research V (Fig. 1). The exact longitudes of the eight sampling stations from number 1 to 8 are 121.74°E, 121.25°E, 123°E, 124°E, 125°E, 126°E, and 128°E, respectively. It should be noted that all of the size-fractionated plankton samples for the 2014 spring cruise were collected at Sta. 6 with high vertical sampling resolution ranging from the surface to 200 m (Table 1). We have also collected suspended particles from surface water at Sta. 1, 5, and 7 in the 2013 cruise through a trace metal clean surface pump installed in front of the research vessel (Table 1). Along with size-fractionated particles, the information on trace metal concentrations or fluxes for seawater, sinking particles, and aerosols are available for the other two cruises. In addition to the two GEOTRACES cruises, the third cruise was carried out in November 2013 at six stations, including Sta. 1 and 3 and the other two Kuroshio stations, Sta. A (121.5°E, 22.5°N) and

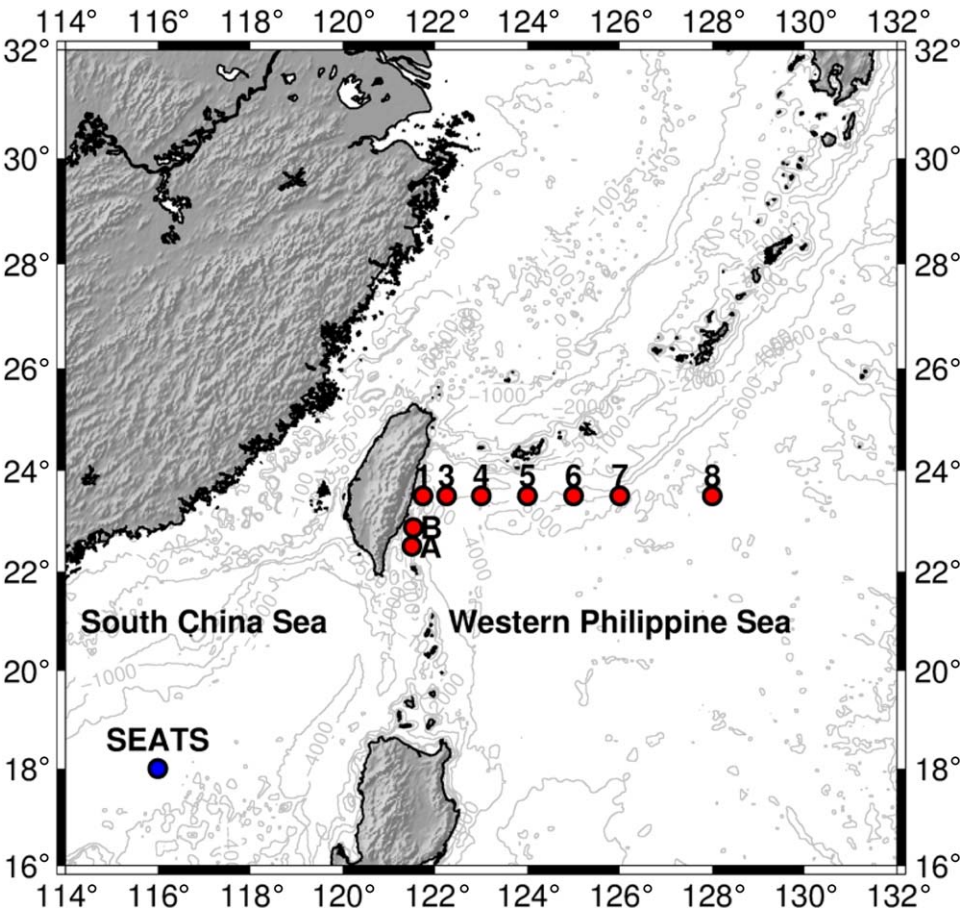


**Fig. 1.** The sampling stations of this study in the WPS and the Kuroshio region, shown as red circles. The data previously obtained from Taiwan time series station in the South China Sea, South East Asia Time-Series Station (SEATS), are also shown in this study for comparison. [Color figure can be viewed at wileyonlinelibrary.com]

B (121.53°E, 22.87°N) via R/V Ocean Research I (Fig. 1). The detailed sampling information, including time, stations, depths, mixed layer depth and chlorophyll *a* (Chl *a*) maximum depths of the stations, and filtration volume, are shown in Table 1.

A trace metal clean filtration device equipped with 150 $\mu$m, 60 $\mu$m, and 10 $\mu$m aperture changeable Nitex nets in sequence was used to filter and concentrate the size-fractionated plankton samples by gravity. The detailed information for the filtration apparatus is described in the patent of Wen et al. (2005) and the study of Ho et al. (2007). The details of the sampling procedures are briefly described here. Seawater was collected using acid-washed 12 L Teflon-coated Go-Flo bottles (General Oceanics) mounted on a Teflon-coated rosette equipped with stainless hydro-wires. Before sampling, six acid-washed clean C-flex tubes were connected to the water outlets of the Go-Flo bottles and the polytetrafluoroethylene (PTFE) inlet of the filtration apparatus. Then, all of the seawater in the bottles was released from the Go-Flo bottles through the tubes to the filtration apparatus in a fully closed system to prevent contamination (Ho et al. 2007). The seawater level in the apparatus was kept high so that size-fractionated planktons were gently sieved through the nets and sank into the acid-washed 100 mL polyethylene bottles mounted at the bottom of the nets by gravity. The live plankton observed in the sampling bottles demonstrates the gentleness of the gravitational process through the filtration apparatus (https://www.youtube.com/watch?-v=aLdvRJLUXlM). With a large surface net area, it took less than 20 min to filter more than 200 liters of seawater collected by Go-Flo bottles. Tubing connected to the surface pump was all Teflon tubing. The outlet of the pumping water was connected to the filtration apparatus with size-fractionated nets. The concentrated plankton samples collected in the 100 mL polyethylene bottles were then filtered again through an acid-washed 47 mm plastic filter holder with 10 $\mu$m pore size acid-washed polycarbonate membranes in a trace metal clean laminar flow bench on board.

The seawater passed through the net filtration apparatus was also collected in acid-washed polypropylene carboys to obtain the smallest size plankton fraction (0.2–10 $\mu$m). Before filtration, the seawater in the carboys was gently

**Table 1.** Sampling information for size-fractionated plankton collected in this study, including sampling seasons, stations, depths, mixed layer depth and chlorophyll *a* maximum depths of stations, and filtration volume for each size fraction.

| | | | | | Filtration volume (L) | |
|---|---|---|---|---|---|---|
| Sampling season | Sampling station | Depth (m) | Mix layer depth (m) | Chl *a* maximum depth (m) | 0.2–10 $\mu$m | All other size fractions |
| Jul 2013 (summer) | 1 to 3* | 5 | 25 | 25 | 6 | 135 |
| | 3 | 70 | 25 | 70 | 6 | 240 |
| | 4 | 85 | 60 | 85 | 6 | 240 |
| | 5 to 6* | 5 | 70 | 85 | 6 | 135 |
| | 8 to 7* | 5 | 65 | 80 | 6 | 240 |
| | 7 | 80 | 70 | 80 | 6 | 240 |
| | | 150 | | | 6 | 135 |
| Nov 2013 (Autumn) | A | 35 | 30 | 50 | 10 | 220 |
| | | 150 | | | 10 | 200 |
| | B | 30 | 50 | 50 | 10 | 100 |
| | | 50 | | | 10 | 220 |
| | | 150 | | | 10 | 220 |
| | 1 | 45 | 50 | 45 | 10 | 220 |
| | | 150 | | | 10 | 220 |
| | 3 | 110 | 70 | 110 | 10 | 160 |
| | | 150 | | | 10 | 220 |
| Mar 2014 (Spring) | 6 | 10 | 50 | 85 | 18 | 262 |
| | | 35 | | | 19 | 222 |
| | | 85 | | | 20 | 232 |
| | | 150 | | | 20 | 232 |

* Samples were collected by using trace metal clean surface pump.

mixed. Approximately 6–20 L of the filtered seawater was further filtered by an acid-washed polypropylene filter holder with 0.2 $\mu$m acid-washed polyethersulfone membranes. Vacuum pressure was kept under 15 KPa to reduce cell breakup during the filtration, as suggested by GEOTRACES recommended protocol (Cutter et al. 2014). The particles on all the membranes were quickly rinsed and misted with Milli-Q water three times to remove seawater residue to decrease the interference of sea salts on trace metal analysis. The rinsing and misting step is essential for inductively coupled plasma mass spectrometry (ICPMS) analysis to remove seawater matrix in samples. The rinsing step was kept to about 1 s each time to reduce the impact on phytoplankton. The total volume filtered for the size fraction ranging from 0.2 $\mu$m to 10 $\mu$m ranged from 6 L to 20 L (Table 1). In terms of the three larger fractions, we filtered seawater with volumes ranging from 135 L to 262 L to obtain sufficient biomass for measurement (Table 1). The polycarbonate membranes with concentrated plankton particles were stored in acid-washed 15 mL Teflon vials with screw caps and were stored in an on-board freezer. All the samples were brought back to a land-based laboratory for further pretreatment and analysis.

**Analytical methods**

Detailed information of analytical methods, including precision, accuracy, and detection limits for marine plankton analysis, are described in the studies of Ho et al. (2003) and Ho et al. (2007). In brief, the frozen filters were freeze-dried first under trace metal clean condition to remove water content. The membranes were then digested in 15 mL acid-washed Teflon vials by refluxing the acid solution that contained with 5 mL 8 N super pure $HNO_3$ and 2.9 N super pure HF mixture at 120°C on a hot plate for 12 h. In the digestion process, the membrane was attached to vial wall with sample side facing out for digestion (Cullen and Sherrell 1999). After the digestion, we took out the membranes by using acid-washed Tefzel forceps in a trace metal clean hood and used 2 mL Milli-Q water to rinse each membrane right above the digestion vial to collect the rinsing solution in the vial. The digested solution was then evaporated on hot plate at 80°C in a trace-metal clean hood until near dryness. The samples were then re-dissolved with 1 mL concentrated super pure $HNO_3$ and was evaporated to near dryness again. The dried samples were re-dissolved by adding 5 mL 0.5 N super pure $HNO_3$. In general, a further 10-fold dilution of the 5 mL

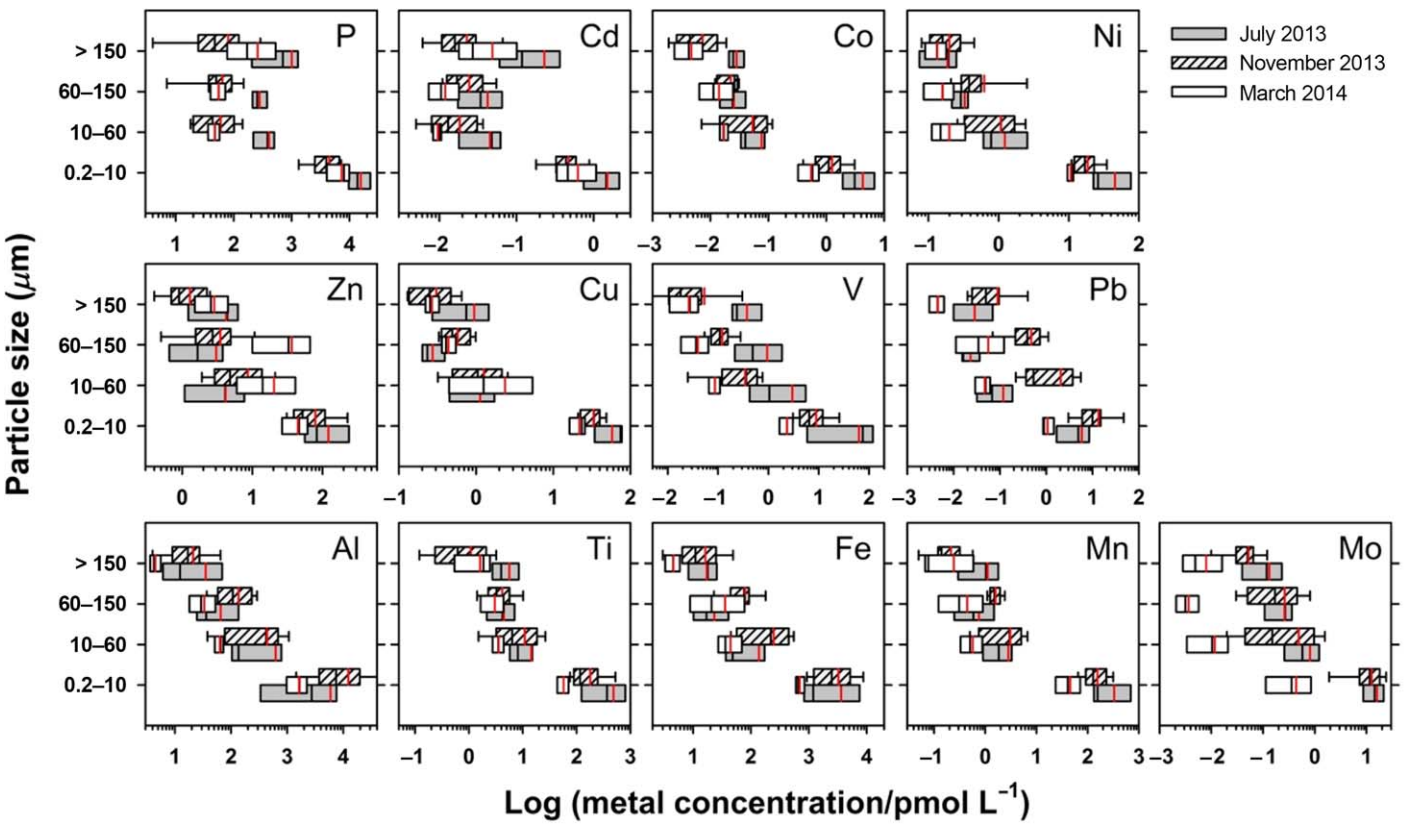


**Fig. 2.** The temporal variations of trace metal concentrations in size-fractionated suspended particles and plankton collected in the WPS, which include fractions of 0.2–10 $\mu$m, 10–60 $\mu$m, 60–150 $\mu$m, and $>150$ $\mu$m. For the data from July 2013 and March 2014, the ends of boxes represent the 5$^{th}$ and 95$^{th}$ percentiles of the data set. Due to limited data points, the ends of boxes and whiskers represent the 25$^{th}$ and 75$^{th}$ percentiles and the 5$^{th}$ and 95$^{th}$ percentiles for the data from November 2013, respectively. The median and the mean are presented by the black and red lines, respectively. [Color figure can be viewed at wileyonlinelibrary.com]

samples was needed for ICPMS analysis. All of the samples were analyzed by a sector field ICPMS (Element XR, Thermo Fisher Scientific), coupled with a flow injection auto-sampler with a 2 mL sample loop (SC-Fast, Elemental Scientific). Dry plasma mode was used to reduce oxide and hydride interferences through an Apex HF-Spiro membrane desolvation device (Elemental Scientific). Signal sensitivity was tuned to one million counts per second for 1 ppb $^{115}$In under low resolution, with signal stability around 1% and oxide level below 0.5%. The isotopes $^{111}$Cd, $^{112}$Cd, $^{207}$Pb, and $^{208}$Pb were analyzed at low resolution (M/$\Delta$M $\sim$ 300), and $^{27}$Al, $^{47}$Ti, $^{51}$V, $^{31}$P, $^{54}$Fe, $^{55}$Mn, $^{56}$Fe, $^{59}$Co, $^{60}$Ni, $^{61}$Ni, $^{63}$Cu, $^{64}$Zn, $^{65}$Cu, $^{66}$Zn, $^{95}$Mo, and $^{97}$Mo were determined in medium resolution mode (M/$\Delta$M $\sim$ 5000). The accuracy of the pretreatment and analytical procedures of this study was validated by measuring biological reference material, BCR-414. The recovery for the certified elements generally ranges from 85% to 105% (Supporting Information Table S1). The information of the overall procedure blanks and detection limits of the method are shown in the Supporting Information Table S2. In summary, all of the metal concentrations in the processed samples for ICPMS analysis were at least one order of magnitude higher than the concentrations of procedural blanks and detection limits (Supporting Information Table S2).

## *Results and discussions*

### Trace metal concentrations in size-fractionated plankton

The trace metal concentrations of size-fractionated plankton samples collected in this study, including 0.2–10 $\mu$m, 10–60 $\mu$m, 60–150 $\mu$m, and $>150$ $\mu$m, are compiled and shown in the Fig. 2. The elemental concentrations vary significantly among different plankton fractions, with concentrations ranging from $10^{-2}$ pmol L$^{-1}$ to $10^{4}$ pmol L$^{-1}$ in the sequence of P$\sim$Al$\sim$Fe $>$ Ti$\sim$Mn$\sim$Zn $>$ Ni$\sim$Pb$\sim$Cu$\sim$V $>$ Mo $>$ Co$\sim$Cd (Fig. 2). The concentrations of most elements in the smallest fraction, 0.2–10 $\mu$m, were one to two orders of magnitude higher than the concentrations in other larger fractions. P concentrations were relatively comparable among the three larger fractions, and the concentrations were about two orders of magnitude lower than the smallest fraction. Similar patterns are observed for Cd, Co, Ni, and Mn. Compared to P concentrations in three larger fractions, Al

concentrations in the three larger fractions increased with decreasing plankton sizes. Some metals exhibit a similar size-associated distribution trend to Al, including Ti, V, Fe, Co, Zn, Mo, and Pb. Temporal variations are also significant for some of the elements. The concentrations of P, Cd, and V observed in the summer cruise are significantly ($p < 0.01$) higher than the other two cruises for all fractions. The Mo concentrations observed in July and November cruises were also significantly higher than the March cruise. The Pb concentrations in November cruise were higher than the other two cruises. The concentrations obtained in the relatively nearshore stations (Sta. A, B, 1–3) are compared with the concentrations obtained in the offshore stations (Sta. 4–8) (Supporting Information Fig. S1). We found that the concentrations of some metals, including Al, Fe, Mn, and Pb, are generally higher in the nearshore stations than the offshore stations.

**Using elemental ratios to identify trace metal sources**

Elemental ratios, normalized to major elements in biotic or abiotic particles, are useful indicators in elucidating external sources of trace metals and their internal transformation processes in marine suspended particles and plankton (Ho et al. 2007). Based on the elemental metal to P and Al ratios in suspended particles, our previous studies in the SCS have identified three major metal components in the suspended particles, including an anthropogenic aerosol component, lithogenic particles, and a plankton intracellular pool. Depending on their physicochemical property and interaction with plankton, particulate trace metals originating from various metal sources may be categorized into the three different groups. Using Fe, Cd, and Zn as examples, particulate Fe in the surface water of the SCS mostly originates from abiotic particles, either extracellularly adsorbed and aggregated on the plankton or independently existing as abiotic particles. In contrast to Fe, particulate Cd in the surface water mainly originates from the deposition of anthropogenic aerosols and exists in plankton intracellular pool (Ho et al. 2009, 2010). Similar to Cd, Zn also originates from anthropogenic aerosol deposition in the SCS surface water. Although the majority of aerosol Zn is also highly soluble like Cd, most of the Zn are eventually adsorbed or aggregated extracellularly on plankton instead of being taken up by plankton (Ho et al. 2007, 2010).

Here, we have applied a similar approach used in the SCS studies to investigate trace metal sources and transformation processes in the size-fractionated plankton and suspended particles collected in the WPS. Our previous SCS studies have demonstrated that bulk particulate P concentrations serve as an appropriate proxy for plankton biomass. Through microscopic examination, we have confirmed that the suspended particles larger than 10 $\mu$m in the surface water are all composed of plankton cells and biogenic particles (Ho et al. 2007). Using typical lithogenic P to Al ratio, 7 mmol mol$^{-1}$ (Hu and Gao 2008), to estimate lithogenic P, lithogenic P accounts for less than 1% of the P in the 0.2–10 $\mu$m fraction particles in the WPS. Thus, bulk particulate P represents plankton biomass so that metal to total particulate P ratios may be used to quantitatively evaluate the contribution of intracellular metals. Through in situ aerosol measurement in the WPS, we found that the P to Al ratio is around 27 mmol mol$^{-1}$ in the aerosols. Assuming that the aerosols and lithogenic particles account for half of abiotic P, the estimated abiotic P would account for only 5% of total particulate P or biogenic P account for 95% of total particulate P. Total particulate P measured in the plankton assemblages is thus mainly biogenic and intracellular.

In terms of abiotic components, we can use the significantly different metal to Al ratios between anthropogenic aerosols and lithogenic particles to examine the relative influence of the two abiotic sources controlling upper water column particulate metal composition of the region. It is well known that metal to Al ratios in lithogenic particles exhibit relatively constrained value with limited variations. Here, we use the average metal to Al ratios obtained from related studies in East Asia, which were compiled by the study of Hu and Gao (2008) as reference lithogenic ratios (Table 2). We have used the averaged metal to Al ratios in aerosols collected in this study to represent the component of anthropogenic aerosols (Table 2). We have observed that metals to Al ratios in the aerosol samples are relatively constrained among different stations and different seasons in the WPS. The metal enrichment factors in aerosols are calculated by aerosol metal to Al ratios divided by metal to Al ratios in lithogenic particles. These are shown in Table 2 to exhibit the differences of the factors among the metals determined. Aside from Ti, Mn, Fe, and Co, most of trace metal ratios in the aerosol samples are one to two orders of magnitude higher than the ratios in lithogenic particles.

We thus assume that particulate trace metals obtained in the surface water of the WPS are composed of three major components as observed in the SCS, two abiotic components originating from anthropogenic aerosol deposition or lithogenic particles, and an intracellular pool in plankton as the third component. Total metal concentrations in the suspended particles are thus quantitatively expressed as following mass balance formula.

$$[M]_t = a[Al]_a + b[Al]_l + c[P]_t$$

$a$: Al-normalized metal ratios in aerosols (shown as red lines in figures)

$b$: Al-normalized metal ratios in nonaerosol lithogenic particles (shown as blue lines)

$c$: P-normalized metal quota in plankton (shown as green lines)

$[M]_t$: total particulate metal concentration of individual element

$[Al]_a$: Al concentration in anthropogenic aerosol particles

**Table 2.** Comparison of the metal to Al ratios (M/Al) of the WPS aerosol samples with the metal to Al ratios in crustal material (Hu and Gao 2008). The uncertainty of the aerosol ratios stands for one standard deviation. The enrichment factors in aerosols are calculated by metal to Al ratios in aerosols divided by the crustal ratios.

| | M/Al (mmol mol$^{-1}$) | | |
|---|---|---|---|
| Element | In situ WPS aerosol | Crustal ratios | Enrichment factor |
| Cd | 0.11 ± 0.07 | 0.00027 ± 0.00020 | 407 |
| Mo | 0.28 ± 0.23 | 0.0017 ± 0.0010 | 165 |
| Zn | 27 ± 22 | 0.36 ± 0.12 | 75 |
| Pb | 3.6 ± 2.2 | 0.054 ± 0.037 | 67 |
| Cu | 5.1 ± 3.6 | 0.12 ± 0.07 | 43 |
| Ni | 2.5 ± 1.3 | 0.15 ± 0.11 | 17 |
| V | 5.7 ± 3.0 | 0.64 ± 0.39 | 8.9 |
| Mn | 9.1 ± 3.2 | 3.6 ± 1.8 | 2.5 |
| Co | 0.14 ± 0.05 | 0.068 ± 0.037 | 2.1 |
| Fe | 280 ± 68 | 218 ± 92 | 1.3 |
| Ti | 34 ± 6 | 27 ± 12 | 1.3 |

$[Al]_l$: Al concentration in nonaerosol lithogenic particles

$[P]_t$: total particulate P concentration, assuming that it is biogenic and intracellular P

Conceptually, we may separate bulk abiotic components to total aerosol particles and nonaerosol lithogenic particles in the formula. However, in practice, it is unlikely to be able to differentiate the two individual Al fractions from the two different abiotic components in the particulate samples. To present the data in figures, we sum up the two abiotic fractions first by using bulk particulate Al concentration, $[Al]_t$. Since metal to Al ratios for many elements differ significantly between lithogenic particles and anthropogenic aerosols as mentioned previously, the distribution pattern of metal to Al ratios may exhibit the relative contribution of the two different abiotic components by comparing their elemental ratios in samples to their contrasting reference ratios. Subsequently, we then simplify the three-component mass balance formula into two components, total abiotic and plankton intracellular components.

$$[M]_t = S[Al]_t + c[P]_t$$

$S$: the slopes of the regression lines between M/P and Al/P in Fig. 4

$[Al]_t$: total aluminum concentration in particulate samples

To compare P-normalized or Al-normalized ratios in the samples with the three reference metal ratios, the two-component formula is further transformed into the following formats by dividing the formula with either $[Al]_t$ or $[P]_t$.

$$[M]_t/[Al]_t = S + c[P]_t/[Al]_t \text{ or } [M]_t/[P]_t = S[Al]_t/[P]_t + c$$

Due to dramatic elemental ratio variation in the samples from different depths, stations, and seasons, we present the ratios by using log scales for both x and y axes in the figures with y scales using the same orders of magnitude for the elements whenever possible (Figs. 3, 4). Using log $[M]_t/[Al]_t$ or log $[M]_t/[P]_t$ as y axes and log $[P]_t/[Al]_t$ or log $[Al]_t/[P]_t$ as x axes, respectively, the variability and distribution patterns of the elemental ratios in the samples are presented to evaluate the relative contribution of abiotic or biotic components in the suspended particles and size-fractionated plankton (Figs. 3, 4). Three reference lines, representing metal to Al ratios in aerosols collected in situ, and metal to Al ratios in lithogenic particles, and intracellular plankton quota, are plotted together with P-normalized or Al-normalized elemental ratios in the size-fractionated particulate samples (Figs. 3, 4). The regression lines between log $[M]_t/[Al]_t$ and log $[P]_t/[Al]_t$ or between log $[M]_t/[P]_t$ and log $[Al]_t/[P]$ are also exhibited to evaluate the association between the data and the reference lines (Figs. 3, 4). The extent of association between the three major components may be quantified by using the regression slopes (black dashed lines) with their M/P or M/Al composition in the three major components (Figs. 3, 4). On the grounds that the elemental ratios of intracellular quota and the elemental ratios in the two abiotic components are assumed to be constants, the slopes of intracellular metal quota shown in Fig. 3 and the slopes of abiotic metal composition in Fig. 4 all become 1 after log transformation. The slopes of the data regression lines become the association extent with the three major components respectively (Table 3). Larger slopes suggest greater association with the plankton particles, either intracellularly or extracellularly (Fig. 3). Based on the closeness or association of the elemental ratios to the reference lines (Figs. 3, 4), the distribution patterns of the metals studied can be categorized into three major groups: elements closely associated with biogenic phases (P, Cd, Co, Ni), elements closely associated with anthropogenic aerosols (Zn, Cu, V, Pb, Mo), or elements closely associated with lithogenic phases (Al, Ti, Fe, Mn).

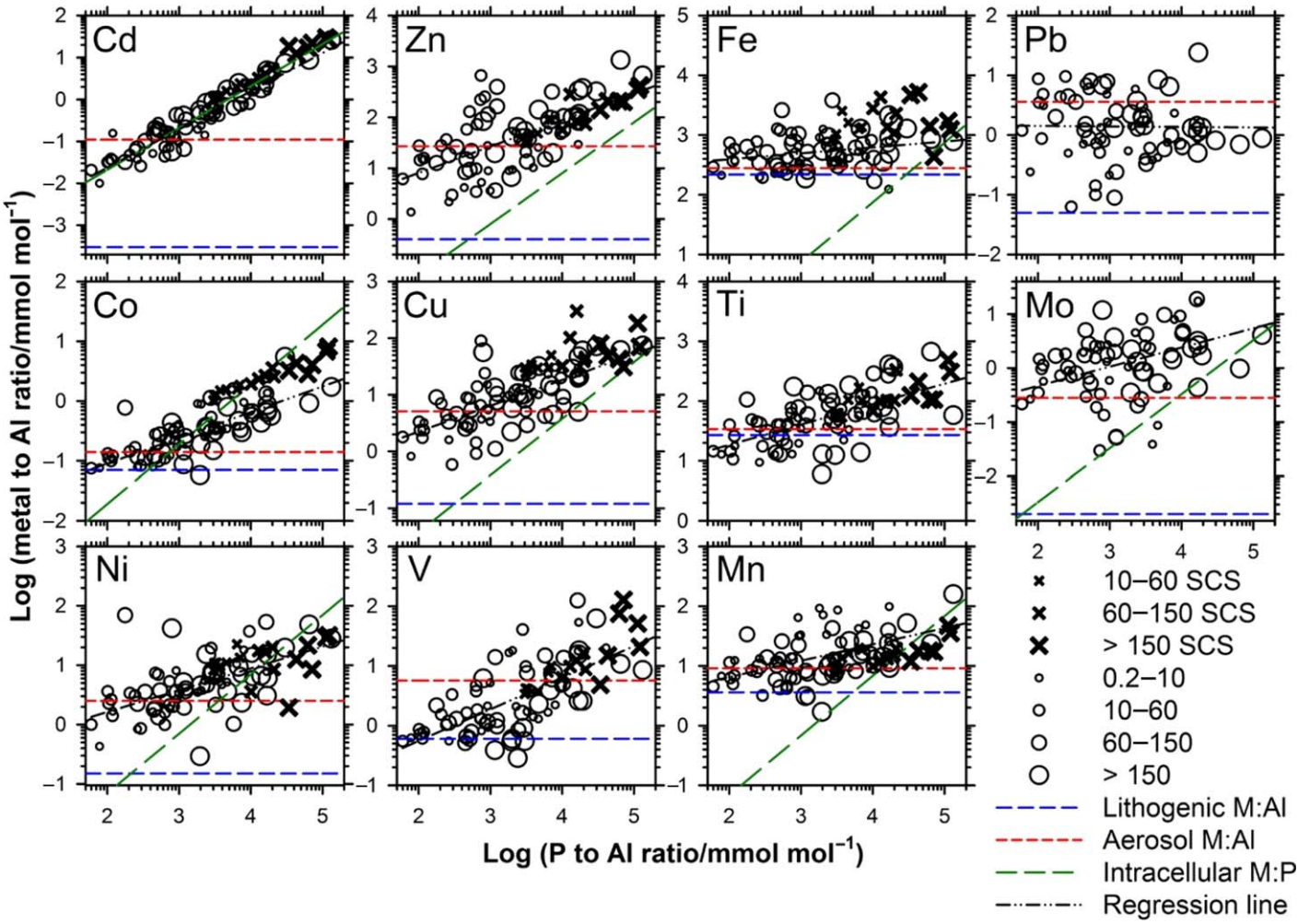


**Fig. 3.** The distribution patterns of trace metal ratios, shown by log M/Al ratios vs. log P/Al ratios, in the size-fractionated suspended particles collected in the WPS. The red and blue parallel dashed lines represent the log M/Al ratios of in situ aerosols collected in the WPS and lithogenic materials (Hu and Gao 2008), respectively. The green dashed lines represent the average metal quotas in marine plankton assemblages, with Fe, Zn, Cu, Co, and Cd quotas cited from Ho et al. (2003) and Mn and Ni quotas from Ho (2006). The intracellular values of Ti, V, and Pb remain unknown. The data shown as cross symbols represent the elemental ratios in the size-fractionated particles and plankton collected in the SCS (Ho et al. 2007). The black dashed lines are regression lines for the data obtained in the WPS. [Color figure can be viewed at wileyonlinelibrary.com]

**Elements closely associated with biogenic phases (P, Cd, Co, Ni)**

The distribution of P-normalized ratios are highly varied for most of the metals studied (Figs. 4, 5). In comparison with known metal intracellular quotas, the P-normalized ratios of Cd, Co, and Ni are relatively constrained and close to their intracellular quotas (Fig. 4), indicating that relatively high percentages of the metals exist in the intracellular pool for the samples. In particular, the P-normalized ratios of Cd exhibit the closest relationship with its intracellular quota among all elements studied (Table 3), with the highest association slope and least offset between data regression line and intracellular reference line (Fig. 3). Indeed, up to 93% of the Cd/P ratios ranged from 0.06 mmol mol$^{-1}$ to 0.36 mmol mol$^{-1}$ to P, with an overall average calculated to be $0.21 \pm 0.15$ mmol mol$^{-1}$ P (Fig. 5). Statistically, this is the same as the intracellular averaged Cd quota and the range proposed, $0.21 \pm 0.22$ mmol mol$^{-1}$ to P (Ho et al. 2003; Ho 2006). Thus, Cd in size-fractionated plankton is mainly intracellular, which is similar to what we have observed in the plankton collected in the SCS (Fig. 3). Despite highly varied Cd/P ratios observed among different marine phytoplankton species and phyla (Ho et al. 2003), averaged Cd/P ratios in the plankton assemblages are comparable to dissolved Cd/P ratios in deep oceanic waters (Ho et al. 2003). The global consistency of Cd to P ratios in plankton assemblages strongly support the concept that metal stoichiometry stands for Cd in the ocean and the Redfield ratio can be reasonably extended to Cd (Ho et al. 2003).

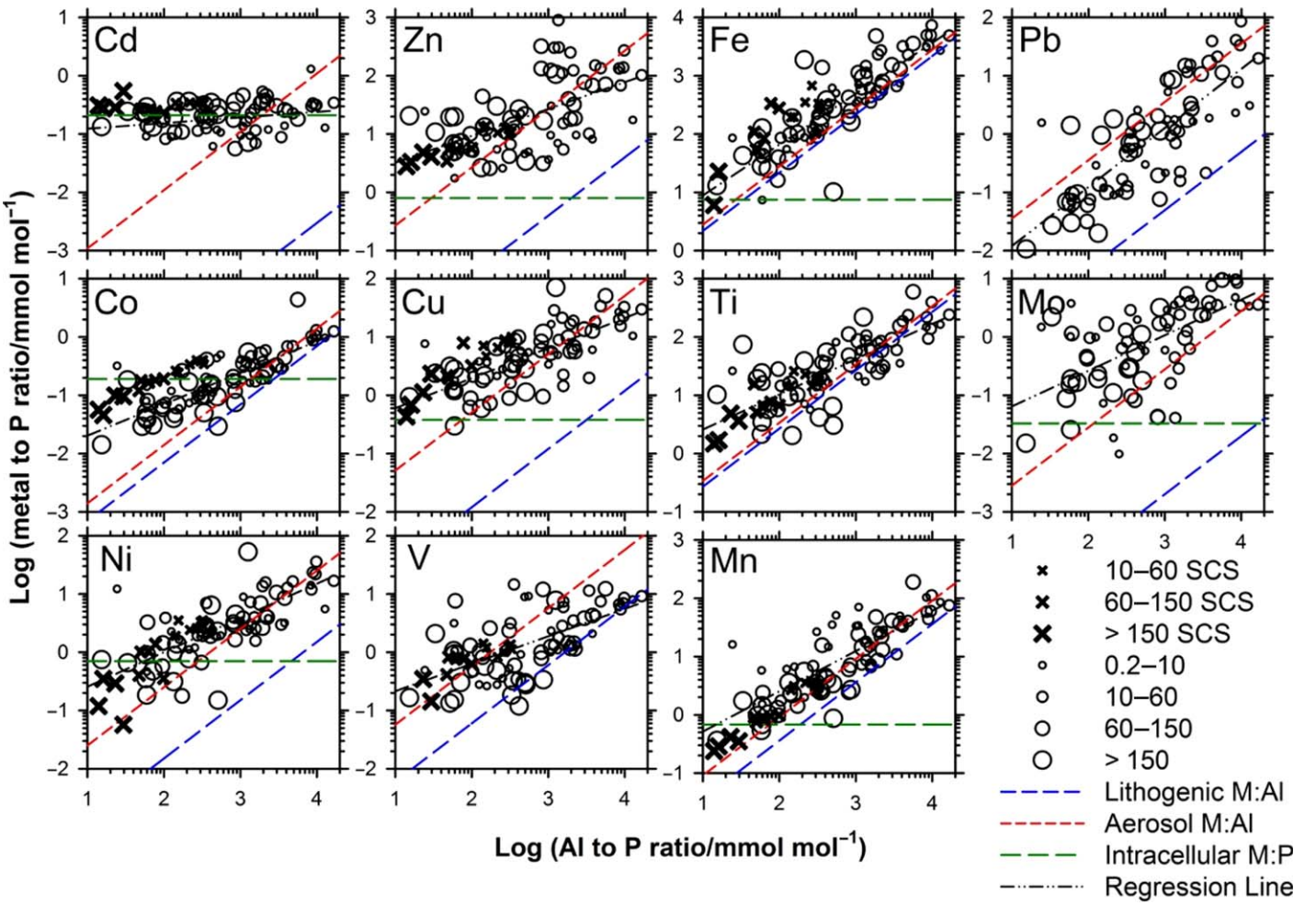


**Fig. 4.** The distribution patterns of trace metal ratios, shown by the log M/P ratios vs. log Al/P ratios, in all of the size-fractionated suspended particles collected in the WPS. The three reference lines represent the same biotic and abiotic ratios as shown in Fig. 3. [Color figure can be viewed at wileyonlinelibrary.com]

The Cd stoichiometry can be attributed to the coupling effects of low Cd flux but high uptake in the euphotic zone and its relatively low particle reactive property. It should be noted that absolute Cd concentrations are extremely low in both lithogenic dusts and anthropogenic aerosols (Table 2). However, laboratory studies show that Cd uptake rates by diatom and coccolithophore are relatively high and can be up to 1–100 $\mu$mol mol C$^{-1}$ d$^{-1}$, particularly under low Fe or low Zn status (Sunda and Huntsman 2000). Cd uptake rates indeed are similar or even higher than Zn uptake rates under seawater with the same inorganic Cd and Zn concentrations for coccolithophore and diatom (Sunda and Huntsman 2000). Estimated by aerosol concentrations, the average aerosol Cd flux was up to 1.1 $\mu$mol m$^{-2}$ yr$^{-1}$ in the surface water of the WPS during our sampling time. The highly soluble aerosol Cd is thus quickly taken up by phytoplankton in the surface water of the WPS.

Although Cd/P ratios exhibit strong association with its intracellular reference line (Table 3), the ratios of the smallest size fraction are significantly lower than the ratios observed in other larger fractions (Fig. 5). It is expected that phytoplankton in the smallest fraction may possess relatively low Cd quota, as laboratory studies show that cyanobacteria are most sensitive to Cd toxicity among major phytoplankton groups (e.g., Payne and Price 1999). The major phytoplankton groups in the smallest fraction, 0.2–10 $\mu$m, are mainly composed of *Prochlorococcus* and *Synechococcus* in the WPS (Yang 2009). The distinguishable Cd elemental and isotopic ratios among size-fractionated plankton may have the

**Table 3.** Slopes of data regression lines shown in Fig. 3 (log [M/Al] vs. log [P/Al]) to indicate relative association with biogenic particles. The higher the ratio, closer the association with biogenic particles.

| Element | Cd | Zn | V | Cu | Co | Mo | Ni | Ti | Mn | Fe | Pb |
|---|---|---|---|---|---|---|---|---|---|---|---|
| Ratios | 0.91 | 0.53 | 0.52 | 0.47 | 0.46 | 0.45 | 0.41 | 0.38 | 0.27 | 0.13 | 0.0011 |

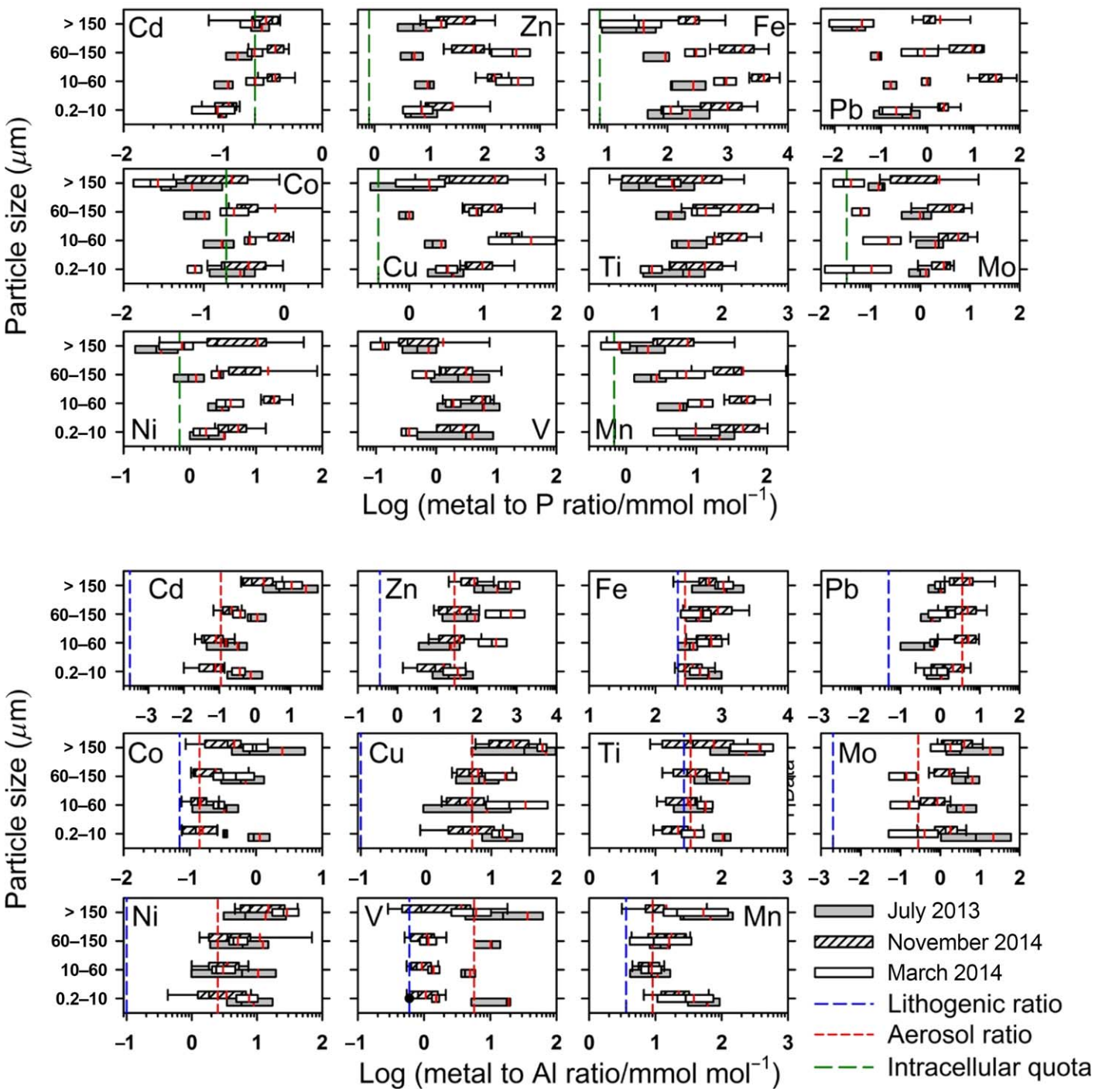


**Fig. 5.** Elemental ratios of the size-fractionated particles collected in this study, shown as log M/P (upper panel) or log M/Al (lower panel) and their comparison to biotic and abiotic reference lines. The reference lines are the same as the ones described in Fig. 3. For the data from July 2013 and March 2014, the ends of boxes represent the 5$^{th}$ and 95$^{th}$ percentiles of the data set. For the data from November 2013, the ends of boxes and whiskers represent the 25$^{th}$ and 75$^{th}$ percentiles and the 5$^{th}$ and 95$^{th}$ percentiles, respectively. The median and the mean are presented by the black and red lines, respectively. [Color figure can be viewed at wileyonlinelibrary.com]

potential to be developed as useful proxies to study particle transformation dynamics.

Co and Ni are known essential trace metals in many marine phytoplankton, particularly in cyanobacteria. The major biological demand for Co is mainly associated with cobalamin ($B_{12}$), an essential organic growth factor required in several biochemical processes. $B_{12}$ is a cofactor of several enzymes such as methylmalonyl-CoA mutase, methionine

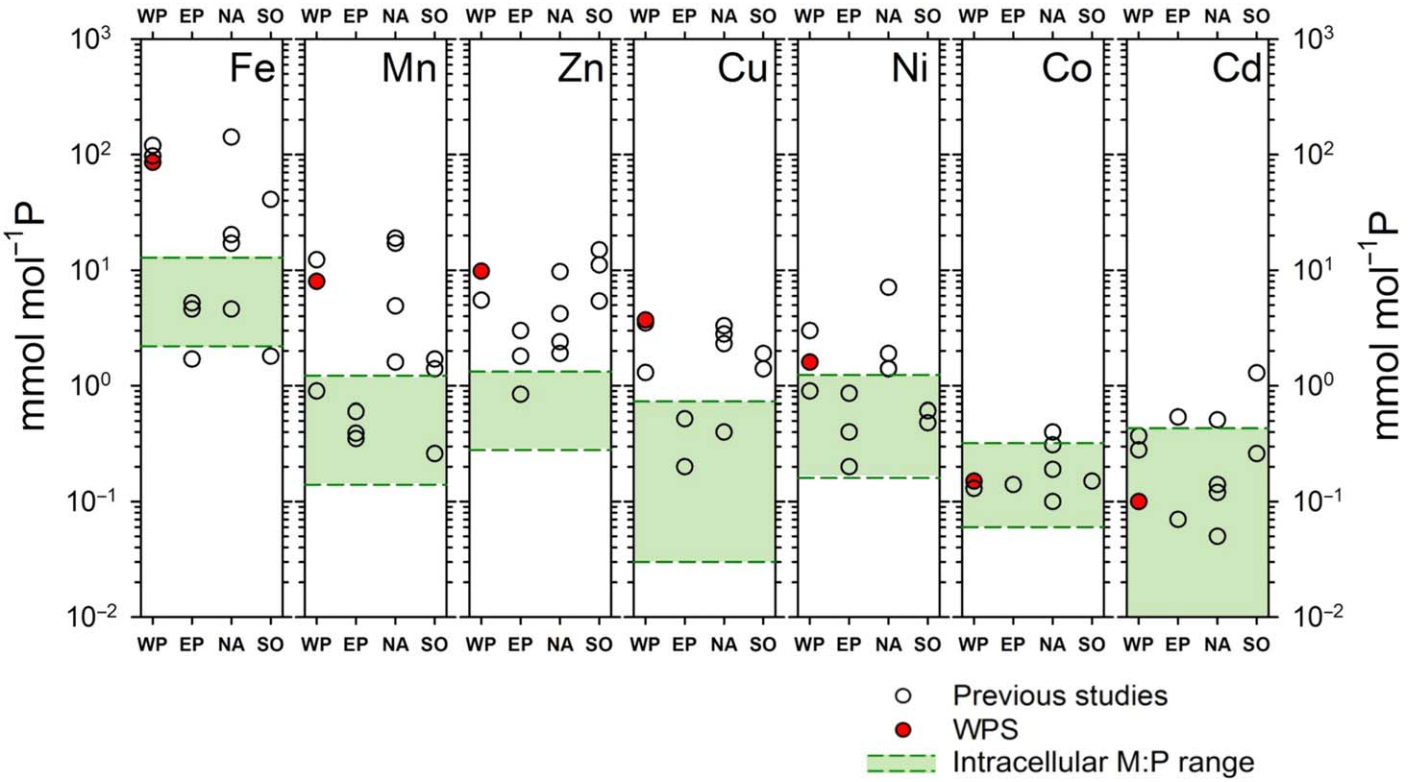


**Fig. 6.** Comparison of trace metal quotas in marine plankton assemblages or suspended particles collected in the surface water (< 200 m) of various oceanic regions globally with intracellular trace metal composition. The highlighted green areas within the two green dashed lines represent the ranges of averaged intracellular trace metal quotas with one standard deviation, as $P_{1000}$ $Fe_{7.5 \pm 5.3}$ $Mn_{0.68 \pm 0.54}$ $Zn_{0.80 \pm 0.52}$ $Cu_{0.38 \pm 0.35}$ $Ni_{0.70 \pm 0.54}$ $Co_{0.19 \pm 0.13}$ $Cd_{0.21 \pm 0.22}$ (Ho et al. 2003; Ho 2006). The averaged WPS data obtained in this study are shown as red circles. The oceanic regions include the North Atlantic Ocean (NA), the Eastern Pacific Ocean (EP), the Western Pacific Ocean (WP), and the Southern Ocean (SO). Detailed information of the sampling sites and methods is shown in Table 4. [Color figure can be viewed at wileyonlinelibrary.com]

synthase, and type II ribonucleotide reductase. Marine cyanobacterial genome information indicates that the growth of some *Synechococcus* and all *Prochlorococcus* strains is dependent upon Ni (Dupont et al. 2008). Ni is known to be used in urease and superoxide dismutase (Ni-SOD), which many cyanobacteria possess (Dupont et al. 2008).

Although the majority of P-normalized Co data are close to the intracellular reference line, the overall regression of the ratios are also associated with abiotic references lines (Fig. 4), suggesting that abiotic particles may contribute Co to some extent in the plankton samples. As shown, larger particles tend to have lower Co/P and smaller particles tend to have higher ratios (Figs. 4, 5). It should also be noted that the data near the intercepts of y axes are mainly composed of the largest plankton, zooplankton. Different groups or sizes of plankton would have different biochemical requirements for Co (Sunda and Huntsman 1995; Saito et al. 2002; Rodriguez and Ho 2015). The relatively low Co and Ni quotas in the largest fraction may be explained by their relatively low demands for the two metals, and the relatively high metal quotas in the smallest fraction can be attributed to elevated intracellular requirement of Co and Ni in cyanobacteria. However, the elevated quota in the smaller fractions can also be attributed to increasing cellular surface adsorption or aggregation. The averaged Co/P in the larger plankton is close to their proposed intracellular quota, which is $0.19 \pm 0.13$ mmol mol$^{-1}$ (Ho et al. 2003). Co to P ratio in other oceanic regions also show constrained values similar to the proposed quota, indicating that Co composition in plankton assemblages is relatively constrained in the global ocean (Table 4; Fig. 6). For Ni, the ratios of the samples in some of the two larger fractions are relatively comparable to the intracellular quota, $0.19 \pm 0.13$ mmol mol$^{-1}$ (Ho 2006; Fig. 5), but the Ni/P quotas in other relatively smaller fractions are higher than the intracellular quota. This also suggests the influence of extracellular adsorption or aggregation.

### Elements closely associated with anthropogenic aerosol composition (Zn, Cu, V, Pb, Mo)

The M/Al and M/P ratios of Zn, Cu, V, Pb, and Mo in the size-fractionated plankton are significantly higher than both their corresponding lithogenic M/Al ratio and intracellular M/P quota, shown by the significant offset between their

**Table 4.** Comparison of trace metal quotas in marine plankton or total suspended particles (TSP) collected in the surface water (< 200 m) of various oceanic regions globally, including the Western Pacific Ocean (WP), the North Atlantic Ocean (NA), the Eastern Pacific Ocean (EP), and the Southern Ocean (SO). The sampling and filtration information of the cited studies are briefed in the footnotes.

| Oceanic regions | Sampling site (particle type) | Fe | Zn | Mn | Ni | Cu | Co | Cd |
|---|---|---|---|---|---|---|---|---|
| | | (mmol mol$^{-1}$ P ± 1 standard deviation) | | | | | | |
| | Intracellular Quota*,† | 7.5 ± 5.3 | 0.80 ± 0.52 | 0.68 ± 0.54 | 0.70 ± 0.54 | 0.38 ± 0.35 | 0.19 ± 0.13 | 0.21 ± 0.22 |
| Western | **This Study, WPS** (TSP)‡ | 86 ± 66 | 9.8 ± 7.7 | 8.0 ± 7.8 | 1.6 ± 0.8 | 3.7 ± 2.1 | 0.15 ± 012 | 0.10 ± 0.03 |
| Pacific (WP) | South China Sea (Plankton)§ | 120 ± 90 | 5.5 ± 2.0 | 0.9 ± 0.5 | 0.9 ± 0.5 | 3.5 ± 2.1 | 0.13 ± 0.05 | 0.28 ± 0.08 |
| | Tasman Sea (TSP)‖ | 97 ± 87 | n.a. | 12 ± 11 | 3.0 ± 1.7 | 1.3 ± 0.9 | 0.13 ± 0.09 | 0.37 ± 0.16 |
| North | North Atlantic Ocean (flagellated)¶ | 4.6 ± 1.3 | 1.9 ± 0.69 | 1.6 ± 0.18 | 1.4 ± 0.02 | 0.37 ± 0.06 | 0.19 ± 0.02 | 0.51 ± 0.09 |
| Atlantic (NA) | North Atlantic Ocean (*Tricho.*)#,** | 17 ± 2 | 9.7 ± 4.6 | 4.9 ± 0.4 | 7.1 ± 0.7 | 3.3 ± 0.5 | 0.10 | 0.05 ± 0.01 |
| | Sargasso Sea (TSP)†† | 142 ± 24 | 2.4 ± 1.1 | 17 ± 12 | 1.9 ± 1.8 | 2.8 ± 1.3 | 0.4 ± 0.1 | 0.12 ± 0.03 |
| | North Atlantic transect (labile particulate matter)‡‡ | 20 ± 13 | 4.2 ± 2.2 | 19 ± 16 | 1.4 ± 0.4 | 2.3 ± 1.1 | 0.3 ± 0.1 | 0.14 ± 0.05 |
| Eastern | Monterey Bay (diatom)§§ | 5.2 ± 6.8 | 0.84 ± 0.4 | 0.39 ± 0.21 | 0.20 ± 0.16 | 0.20 ± 0.12 | n.a. | 0.07 ± 0.02 |
| Pacific (EP) | MANOP Site C (zoopl.)‖‖ | 4.6 ± 0.66 | 3.0 ± 1.3 | 0.34 ± 0.04 | 0.86 ± 0.17 | 0.52 ± 0.05 | n.a. | 0.54 ± 0.10 |
| | Around Galapagos (phyto.)¶¶ | 1.7 ± 0.1 | 1.8 ± 0.2 | 0.6 ± 0.1 | 0.4 ± 0.04 | n.a. | 0.14 ± 0.02 | n.a. |
| Southern | Pacific Sector, SOFeX (all cell type)## | 1.8 | 5.4 | 0.26 | 0.61 | n.a. | n.a. | n.a. |
| Ocean (SO) | Crozet Basin (large diatoms)‖‖ | 9.8 ± 3.8 | 15 ± 2.6 | n.a. | 0.48 ± 0.28 | 1.9 ± 0.07 | n.a. | 0.26 ± 0.26 |
| | Ross Sea (large diatoms)*** | n.a. | 11 ± 0.7 | 1.7 ± 0.1 | n.a. | 1.4 ± 0.1 | 0.15 ± 0.01 | 1.29 ± 0.07 |
| | Amundsen Sea (TSP)††† | 41 ± 41 | n.a. | 1.4 ± 1.9 | n.a. | n.a. | n.a. | n.a. |

n.a., not available; phyto, phytoplankton; *Tricho*, *Trichodesmium*; zoopl, zooplankton.
* Ho et al. (2003) (culture study).
† Ho (2006) (field and culture study).
‡ This study, excluded data collected from coastal Sta. 1, 3, A, and B.
§ Ho et al. (2007) (size-fractionated plankton net).
‖ Bowie et al. (2010) (1 μm, pump filtration).
¶ Kuss and Kremling (1999) (pump filtration).
# Tovar-Sanchez et al. (2006) (100 μm, plankton net).
** Nuester et al. (2012) (100 μm, plankton net).
†† Sherrell and Boyle (1992) (1 μm, pump filtration).
‡‡ Twining et al. (2015b) (0.45 μm, pump filtration).
§§ Martin and Knauer (1973) (76 μm, plankton net).
‖‖ Collier and Edmond (1984) (44 μm, plankton net).
¶¶ Twining et al. (2011) (single cell, synchrotron).
## Twining et al. (2004) (single cell, synchrotron).
*** Cullen et al. (2003) (0.45 μm, pump filtration).
††† Planquette et al. (2013) (0.45 μm, pump filtration).

elemental ratios and the known reference lines (Figs. 3-5). However, the elemental ratios also exhibit significant association with the two abiotic reference lines (Fig. 4), indicating that these metals are also associated with the abiotic components. Among the two abiotic sources, the M/Al ratios for the elements are relatively close to the reference lines of anthropogenic aerosols (Figs. 3-5), suggesting that anthropogenic aerosols are possibly the dominant source of these metals in the size-fractionated plankton and suspended particles.

The regression lines of the P-normalized ratios for Zn, Cu, V, and Mo are also associated with the intracellular reference lines (Fig. 3; Table 3). As their P-normalized ratios are significantly higher than their corresponding intracellular quotas, the association of the elemental ratios with intracellular composition may be attributed to extracellularly adsorbed or aggregated particles originating from anthropogenic aerosols. Figure 4 shows that the offsets between the M/P ratios, and the intracellular quota (green lines) decrease with decreasing Al/P ratios. Compared to the other elements in this group, Pb possesses the lowest association ratio to biotic particles, indicating that Pb does not closely associate with biotic materials (Figs. 3, 4).

The intercepts of log M/P on y axes or the lower limit of the M/P ratios provide valuable information to examine phytoplankton intracellular quota proposed in previous studies (Ho et al. 2003; Ho 2006). Although most of the P-normalized ratios for Zn and Cu are higher than their

intracellular quota, the y intercepts of log M/P are relatively close to or approaching intracellular quota (Fig. 4). In terms of Zn, the lowest limit of the Zn/P ratios in the dataset is around 3 mmol $mol^{-1}$ P (Figs. 4, 5), which is still significantly higher the intracellular value observed in laboratory culture experiments, $0.80 \pm 0.52$ mmol $mol^{-1}$ P. The intercept of Cu/P regression line is 0.7 mmol $mol^{-1}$, which is similar to the upper limit of the Cu quota $0.38 \pm 0.35$ mmol $mol^{-1}$ P (Fig. 6). Aside from the data near the intercepts, the majority (> 90%) of the P-normalized Zn and Cu data are significantly higher than their intracellular quota, suggesting that these two metals are mainly extracellularly adsorbed or aggregated on plankton. Applying the same approach on V and Mo, the intercepts of the linear regression lines of the three elements on y axes are about 0.20 mmol $mol^{-1}$ P and 0.065 mmol $mol^{-1}$ P, respectively. These intercepts may be considered as the upper limits of intracellular V and Mo quota in plankton assemblages.

**Elements closely associated with both aerosol and/or lithogenic components (Al, Ti, Fe, Mn)**

For Fe and Ti, the majority of the data are significantly ($p < 0.01$) higher than their M/Al ratios either in aerosol or lithogenic particles. However, the distribution pattern of their Al ratios are relatively close to the two abiotic references in comparison with other metals, with overall ranges varying up to one order of magnitude (Fig. 3). As the ratios of both Fe/Al and Ti/Al in the aerosol and plankton samples are higher than their lithogenic ratios (Table 2), Fe and Ti originating from anthropogenic aerosol deposition are likely to contribute a significant amount of Fe and Ti in the plankton samples. By using a regional air quality model incorporated with an emission module, Lin et al. (2015) indicates that anthropogenic aerosols contribute 62% and 15% of total deposited Fe in summer and spring over the NWPO, respectively. Our aerosol dissolution experiments also show that the averaged Fe solubility of the aerosols collected in the WPS in Milli-Q water ranged from 17% to 11% for summer and spring, respectively. In the Pacific zonal and meridional transect studies, the overall mean aerosol Fe solubility is 9.2% in Pacific Ocean (Buck et al. 2013), also indicating the importance of anthropogenic aerosols as a soluble Fe source in the NWPO and its vicinity. Soluble Fe from aerosols would quickly precipitate as amorphous type iron oxy-hydroxides in oceanic surface water (Zhuang et al. 1990). Fe to P ratios observed in the plankton samples would thus be influenced by the adsorption and aggregation extent originating either from lithogenic crystalline particles or amorphous precipitates. With amorphous Fe oxy-hydroxides adsorbed or aggregated on plankton, the Fe/Al and Fe/P ratios in the particles would then be higher than the elemental ratios in either anthropogenic aerosols or lithogenic particles. In addition to aerosol deposition flux, increasing plankton biomass may also enhance amorphous Fe adsorption and aggregation. Since the amorphous form of iron oxides or oxy-hydroxide provides higher accessibility and bioavailability to phytoplankton than crystalline lithogenic type Fe (Bligh and Waite 2011), the elevated Fe/Al ratios in suspended particles suggest an elevated supply of bioavailable Fe in the euphotic zone of the oceanic region. Overall, the Fe and Ti composition in the plankton assemblages observed in the WPS and the SCS highly contrast to the observation in the North Atlantic Ocean, where the Fe/Al ratios in suspended particles in the top 200 m are relatively close to lithogenic ratios (Sherrell and Boyle 1992; Ohnemus and Lam 2015).

The regression lines of Fe/Al and Ti/Al also exhibit an increasing trend with increasing P/Al ratios (Fig. 3), indicating that the Al-normalized ratios are positively associated with the increasing ratios of biotic to abiotic components or the relative contribution between intracellular and extracellular metals. Plankton size is an important factor causing the association as the extracellularly adsorbed or aggregated metals increase with decreasing sizes. Indeed, we have observed this trend in the SCS datasets (Figs. 3, 4), where samples were all collected at the Chl *a* maximum depth at SEATS stations in the SCS study (Ho et al. 2007). For the WPS data, the trend becomes much less significant as the samples were collected from various stations, depths, and sampling times.

Overall, the distribution pattern of Mn in plankton assemblages is similar with what is observed for Fe and Ti (Figs. 3, 4). As the Mn enrichment factor in aerosols is twofold of Fe (Table 2 and Figure 3), the discrepancy between the two abiotic reference lines for Mn provides better constrains than Fe and Ti to evaluate the relative contribution of the abiotic Mn sources in the plankton assemblages. Since the majority of the Mn/Al data overlap or are close to the reference line of aerosol composition (Fig. 4), anthropogenic aerosols are highly likely to be the major particulate Mn source in the surface water of the WPS. The microbial oxidization of $Mn^{2+}$ to insoluble $MnO_2$ may be the other particulate Mn source in the surface water (Tebo et al. 2004), resulting in the elevation of Mn to Al ratios in some of the samples (Fig. 4).

Although most of the M/P ratios for Fe, Ti, and Mn are profoundly above their intracellular reference lines (Figs. 4, 5), the lower limits or their y intercepts are comparable with their intracellular quotas (Fig. 3). The y intercept of the largest fraction of Fe is around 10 mmol $mol^{-1}$, statistically the same as the proposed intracellular quota, $7.5 \pm 5.3$ mmol $mol^{-1}$ (Ho et al. 2003). Similarly, the lower limit of Mn/P ranges from 0.30 mmol $mol^{-1}$ to 1.0 mmol $mol^{-1}$, also comparable to the proposed intracellular quota, $0.68 \pm 0.54$ mmol $mol^{-1}$ (Fig. 5). The consistency between the observed data and proposed intracellular quota validate the stoichiometry of these metals in plankton assemblages (Ho et al. 2003; Ho 2006). Similar to Co and Ni quotas, the variations of Mn quota among the size-fractionated plankton may be

explained by their biological uptake or cellular surface to volume ratios (Fig. 5).

**Temporal and spatial variations of the elemental ratios**

In terms of the temporal variations of size-fractionated particles, we have observed elevated metal to P ratios during November and March cruises in the two size fractions, 10–160 $\mu$m and 60–150 $\mu$m, for almost all of the elements, except V and Mo (Fig. 5). Since the particles larger than 10 $\mu$m are composed of eukaryotic phytoplankton and zooplankton, the elevated M/P ratios in these two fractions are likely due to preferential extracellular metal adsorption or abiotic particle aggregation. The elevated extracellular adsorption or aggregation of trace metals may also be attributed to the variations of sampling sites among the cruises. It should be noted that the sampling stations are not exactly the same among the three cruises. In particular, the sampling stations of November cruise were all located in the Kuroshio region. Indeed, the M/Al ratios of November cruise are generally lower than the other two cruises, most likely due to the elevated contribution of lithogenic particles in the samples. On the contrary, V/Al ratios were one order of magnitude higher in July (summer) than November and March cruises. V is known to be the most abundant trace metal in heavy oils used (Becagli et al. 2012) and ocean shipping frequency is highest in summer in the NWPO region (Chen et al. 2014). Thus, the emission of fly ash generated from heavy oil burning in container tankers or fishing boats may explain the elevated V observed in summer time. In terms of Mo, *Trichodesmium*, possessing Mo-containing nitrogenase, is known to be a dominant phytoplankton in the WPS during summer time (Chen et al. 2008), which can be a potential cause for the elevated Mo quota observed in the July cruise (Fig. 5).

When we separate the data vertically into three layers, including surface water, Chl *a* max, and 150 m, we found that there were no significant vertical variations in the elemental ratios (Supporting Information Fig. S2). However, when we separated the data into nearshore group (Sta. A, B, and 1–3) and offshore group (Sta. 4–8) based on the difference of Al concentrations of the two groups (Supporting Information Fig. S1), we observed significantly lower P/Al and M/Al ratios at nearshore stations compared to offshore stations (Supporting Information Fig. S3). Overall, the relatively low P/Al and M/Al ratios are most likely attributed to the relatively high concentrations of lithogenic particles at the nearshore stations (Supporting Information Fig. S1). In contrast, the relative contribution of the amorphous precipitates originating from aerosol deposition to the abiotic components increases from the nearshore to offshore stations. Based on the sampling stations or the relative contribution of the two different abiotic particles, the elemental ratios would either be close to the reference line of lithogenic crystalline particles or the reference line of anthropogenic aerosols (Supporting Information Fig. S3, lower panel).

**The impact of anthropogenic aerosol deposition in the NWPO**

In comparison with plankton trace metal quota obtained from other oceanic regions globally, the metal quota of Fe, Mn, Zn, and Cu observed in the plankton collected in the WPS and the SCS rank highest among the global data sets (Fig. 6; Table 4). We found that high aerosol deposition in the two regions results in the elevation of particulate metals but not dissolved trace metal concentrations. Most of the soluble metal concentrations remain relatively comparable among the high and low aerosol deposition seasons (Wang and Ho unpubl.). For example, dissolved Fe concentrations (0.30 nM) in the surface water do not change seasonally in the surface water of the WPS and are similar to the concentration levels observed in other open oceanic regions globally. However, both the suspended particulate trace metal concentrations and metal quota in plankton observed in this study are much higher than the data obtained in other oceanic regions (Fig. 6), including the high lithogenic aerosol deposition oceanic region near the Saharan desert (Twining et al. 2015). Our WPS data suggest that highly soluble trace metals that originate from anthropogenic aerosols are prone to adsorption and aggregation on plankton and may result in a relatively longer residence time in the surface water than trace metals in lithogenic aerosols. Most of the metals measured in the plankton samples, including Fe, Mn, Cu, Zn, and Ni, are significantly higher than their proposed intracellular trace metal quota, except Cd and Co, pointing to the importance of extracellular adsorption or aggregation on plankton in the studied region. Similar to what we have observed in the SCS and the WPS, the P normalized quota of Cd and Co in the global data sets are relatively close to our known intracellular trace metal quota (Ho et al. 2003; Ho 2006). Relatively, global Co quotas exhibit the most constrained range among all of the metals (Fig. 6). Compared to other trace metals, the relatively constrained Cd and Co quota observed globally may be attributed to their extremely low concentrations in both lithogenic particles and anthropogenic aerosols.

On the contrary, most of the Zn/P quotas in different oceanic basins are significantly higher than the intracellular quotas (Fig. 6), suggesting that extracellular adsorption or a scavenging process is a dominant process in regulating Zn cycling in the oceanic surface water. As shown in Figs. 3, 4, both Zn/Al and Zn/P ratios obtained from the SCS and the WPS are close to anthropogenic aerosol composition, indicating that anthropogenic aerosol deposition is the major source of suspended particulate Zn in the surface waters. By deploying sediment traps and aerosol collectors to measure trace metal fluxes in the surface water, our previous SCS study has demonstrated that aerosol deposition is the major Zn source in the SCS surface water (Ho et al. 2010). Similar

to what we have observed for Zn composition in size-fractionated plankton in the SCS, Zn/Al ratios in the WPS indicate close association with biotic particles (Fig. 3 and Table 3), but Zn/P ratios in the WPS were much higher than intracellular Zn quotas in phytoplankton. The plankton associated Zn is most likely to be extracellularly adsorbed or aggregated. Recent studies reported relatively light dissolved Zn isotopic composition in seawater, also suggesting strong Zn adsorption in the euphotic zone (Conway and John 2014; John and Conway 2014). Indeed, our SCS moored trap data showed that Zn/Al and Cu/Al ratios in sinking particles exhibited elevated ratios in comparison with their lithogenic ratios. The Zn/Al ratios mostly ranged from 100 mmol $mol^{-1}$ to 1000 mmol $mol^{-1}$, 5 mmol $mol^{-1}$ to 10 mmol $mol^{-1}$, 1 mmol $mol^{-1}$ to 2 mmol $mol^{-1}$ and the Cu/Al ratios ranged from 5 mmol $mol^{-1}$ to 100 mmol $mol^{-1}$, 0.8 mmol $mol^{-1}$ to 3 mmol $mol^{-1}$, 0.6 mmol $mol^{-1}$ to 1.2 mmol $mol^{-1}$ at 120 m, 600 m, and 3500 m, respectively (Fig. 5; Ho et al. 2011). The elevated ratios in sinking particles suggest that a significant amount of Zn and Cu from anthropogenic aerosols is transported to deep water. With the increasing and lasting aerosol deposition in the oceanic surface water during the past few decades, metal adsorption or aggregation on plankton may have become an important process to regulate metal composition in plankton in the surface water globally, particularly for trace metals with high soluble concentrations in anthropogenic aerosols, such as Zn and Cu.

## Conclusion

This study reports trace metal composition in size-fractionated plankton collected in the WPS. Extending our previous observation that anthropogenic aerosols are the major source of particulate trace metals in the surface water of the SCS (Ho et al. 2007, 2010), we demonstrate that particulate trace metals in the surface water of the WPS, an open ocean region in the NWPO, are also attributed to anthropogenic aerosol deposition. Highly soluble trace metals in the aerosols elevate trace metal to P and Al ratios in the suspended particles and size-fractionated plankton assemblages. The samples with lowest Al/P ratios exhibit comparable metal to P ratios as intracellular quota proposed in plankton assemblages, validating the intracellular metal stoichiometry concept in plankton assemblages. The relatively high trace metal to P or Al ratios observed in the WPS suggest that anthropogenic aerosol deposition have changed particulate trace metal composition in the surface water of the large portion of the NWPO. For Fe, Mn, Cu, and Zn, the highly variable trace metal quota observed in global oceanic regions supports our previous argument that bulk trace metal composition in phytoplankton and zooplankton assemblages are not decided by intracellular components but may mostly be extracellularly adsorbed or aggregated metals, attributed to the influence of aerosol deposition in oceanic surface water (Ho et al. 2007). Observed by moored trap data in the SCS deep water, Zn and Cu to P ratios in sinking particles collected in the deep water are comparable to the elevated metal quota observed in plankton assemblages (Ho et al. 2011), indicating that the biogenic particles with elevated trace metal composition are transported to deep water. How trace metals originating from anthropogenic aerosol deposition have changed trace metal composition in the sub-surface and the deep waters may be revealed by measuring the isotopic and elemental composition of trace metals in aerosols, seawater, suspended and sinking particles in the water column.

## References

Anderson, R. F., and G. M. Henderson. 2005. GEOTRACES: A global study of the marine biogeochemical cycles of trace elements and their isotopes. Oceanography **18**: 76–79. doi:10.1016/j.chemer.2007.02.001

Becagli, S., and others. 2012. Evidence for heavy fuel oil combustion aerosols from chemical analyses at the island of Lampedusa: A possible large role of ships emissions in the Mediterranean. Atmos. Chem. Phys. **12**: 3479–3492. doi:10.5194/acp-12-3479-2012

Bishop, J. K. B., J. M. Edmond, D. R. Ketten, M. P. Bacon, and W. B. Silker. 1977. Chemistry, biology, and vertical flux of particulate matter from upper 400 m of equatorial Atlantic Ocean. Deep-Sea Res. **24**: 511–548. doi:10.1016/0146-6291(77)90526-4

Bligh, M. W., and T. D. Waite. 2011. Formation, reactivity, and aging of ferric oxide particles formed from Fe (II) and Fe (III) sources: Implications for iron bioavailability in the marine environment. Geochim. Cosmochim. Acta **75**: 7741–7758. doi:10.1016/j.gca.2011.10.013

Bowie, A. R., A. T. Townsend, D. Lannuzel, T. A. Remenyi, and P. Van Der Merwe. 2010. Modern sampling and analytical methods for the determination of trace elements in marine particulate material using magnetic sector inductively coupled plasma-mass spectrometry. Anal. Chim. Acta. **676**: 15–27. doi:10.1016/j.aca.2010.07.037

Bruland, K. W., J. R. Donat, and D. A. Hutchins. 1991. Interactive influences of bioactive trace-metals on biological production in oceanic waters. Limnol. Oceanogr. **36**: 1555–1577. doi:10.4319/lo.1991.36.8.1555

Buck, C. S., W. M. Landing, and J. Resing. 2013. Pacific Ocean aerosols: Deposition and solubility of iron, aluminum, and other trace elements. Mar. Chem. **157**: 117–130. doi:10.1016/j.marchem.2013.09.005

Chen, J. M., P. H. Tan, C. M. Hsieh, J. S. Liu, H. S. Chen, L. H. Hsu, and J. L. Huang. 2014. Seasonal climate associated with major shipping routes in the North Pacific and North Atlantic. Terr. Atmos. Ocean. Sci. **25**: 381–400. doi:10.3319/TAO.2013.12.31.01(A)

Chen, Y.-L. L., H.-Y. Chen, S. Tuo, and K. Ohki. 2008. Seasonal dynamics of new production from *Trichodesmium*

$N_2$ fixation and nitrate uptake in the upstream Kuroshio and South China Sea basin. Limnol. Oceanogr. **53**: 1705–1721. doi:10.4319/lo.2008.53.5.1705

Collier, R., and J. Edmond. 1984. The trace element geochemistry of marine biogenic particulate matter. Prog. Oceanogr. **13**: 113–199. doi:10.1016/0079-6611(84)90008-9

Conway, T. M., and S. G. John. 2014. The biogeochemical cycling of zinc and zinc isotopes in the North Atlantic Ocean. Global Biogeochem. Cycles **28**: 1111–1128. doi:10.1002/2014GB004862

Cullen, J. T., and R. M. Sherrell. 1999. Trace metals in small samples of size-fractionated phytoplankton: Collection technique and filter blanks. Mar. Chem. **67**: 233–247. doi:10.1016/S0304-4203(99)00060-2

Cullen, J. T., Z. Chase, K. H. Coale, S. E. Fitzwater, and R. M. Sherrell. 2003. Effect of iron limitation on the cadmium to phosphorus ratio of natural phytoplankton assemblages from the Southern Ocean. Limnol. Oceanogr. **48**: 1079–1087. doi:10.4319/lo.2003.48.3.1079

Cutter, G., P., P. Andersson, L. Codispoti, P. Croot, R. François, M. C. Lohan, H. Obata, and M. Rutgers v. d. Loeff. 2014. Sampling and sample-handling protocols for GEOTRACES cruises. Version 2. Available from http://www.geotraces.org/libraries/documents/Intercalibration/Cookbook.pdf.

Dupont, C. L., K. Barbeau, and B. Palenik. 2008. Ni uptake and limitation in marine *Synechococcus* strains. Appl. Environ. Microbiol. **74**: 23–31. doi:10.1128/AEM.01007-07

Goldberg, E. D. 1954. Marine geochemistry, 1, chemical scavengers of the sea. J. Geol. **62**: 249–265. doi:10.1086/626161

Henderson, G. M., and O. Marchal. 2015. Recommendations for future measurement and modelling of particles in GEOTRACES and other ocean biogeochemistry programmes. Prog. Oceanogr. **113**: 73–78. doi:10.1016/j.pocean.2015.01.015

Ho, T.-Y. 2006. The trace metal composition of marine microalgae in cultures and natural assemblages, p. 271–299. *In* D. V. Subba Rao [ed.], Algal cultures: Analogues of blooms and applications. Science Publishers.

Ho, T.-Y., A. Quigg, Z. V. Finkel, A. J. Milligan, K. Wyman, P. G. Falkowski, and F. M. M. Morel. 2003. The elemental composition of some marine phytoplankton. J. Phycol. **39**: 1145–1159. doi:10.1111/j.0022-3646.2003.03-090.x

Ho, T.-Y., L.-S. Wen, C.-F. You, and D.-C. Lee. 2007. The trace metal composition of size-fractionated plankton in the South China Sea: Biotic versus abiotic sources. Limnol. Oceanogr. **52**: 1776–1788. doi:10.4319/lo.2007.52.5.1776

Ho, T.-Y., C.-F. You, W.-C. Chou, S.-C. Pai, L.-S. Wen, and D. D. Sheu. 2009. Cadmium and phosphorus cycling in the water column of the South China Sea: The roles of biotic and abiotic particles. Mar. Chem. **115**: 125–133. doi:10.1016/j.marchem.2009.07.005

Ho, T.-Y., W.-C. Chou, C.-L. Wei, F.-J. Lin, G. T. F. Wong, and H.-L. Lin. 2010. Trace metal cycling in the surface water of the South China Sea: Vertical fluxes, composition, and sources. Limnol. Oceanogr. **55**: 1807–1820. doi:10.4319/lo.2010.55.5.1807

Ho, T.-Y., W.-C. Chou, H.-L. Lin, and D. D. Sheu. 2011. Trace metal cycling in the deep water of the South China Sea: The composition, sources, and fluxes of sinking particles. Limnol. Oceanogr. **56**: 1225–1243. doi:10.4319/lo.2011.56.4.1225

Hu, Z., and S. Gao. 2008. Upper crustal abundances of trace elements: A revision and update. Chem. Geol. **253**: 205–221. doi:10.1016/j.chemgeo.2008.05.010

Jeandel, C., M. Rutgers van der Loeff, S. Kretschmer, P. J. Lam, R. M. Sherrell, M. Roy-Barman, C. R. German, and F. Dehairs. 2015. What did we learn on the oceanic particle dynamic from the GEOSECS-JGOFS times? Prog. Oceanogr. **133**: 6–16. doi:10.1016/j.pocean.2014.12.018

John, S. G., and T. M. Conway. 2014. A role for scavenging in the marine biogeochemical cycling of zinc and zinc isotopes. Earth Planet. Sci. Lett. **394**: 159–167. doi:10.1016/j.epsl.2014.02.053

Kuss, J., and K. Kremling. 1999. Spatial variability of particle associated trace elements in near-surface waters of the North Atlantic (30°N/60°W to 60°N/2°W), derived by large volume sampling. Mar. Chem. **68**: 71–86. doi:10.1016/S0304-4203(99)00066-3

Lin, Y.-C., J.-P. Chen, T.-Y. Ho, and I.-C. Tsai. 2015. Atmospheric iron deposition in the northwestern Pacific Ocean and its adjacent marginal seas: The importance of coal burning. Global Biogeochem. Cycles **29**: 22–21. doi:10.1002/2013GB004795

Martin, J. H., and G. A. Knauer. 1973. The elemental composition of plankton. Geochim. Cosmochim. Acta **37**: 1639–1653. doi:10.1016/0016-7037(73)90154-3

Nuester, J., S. Vogt, M. Newville, A. B. Kustka, and B. S. Twining. 2012. The unique biogeochemical signature of the marine diazotroph Trichodesmium. Front. Microbiol. **3**: 150. doi:10.3389/fmicb.2012.00150

Ohnemus, D. C., and P. J. Lam. 2015. Cycling of lithogenic marine particles in the US GEOTRACES North Atlantic zonal transect. Deep-Sea Res. Part II Top. Stud. Oceanogr. **116**: 283–302. doi:10.1016/j.dsr2.2014.11.019

Payne, C. D., and N. M. Price. 1999. Effects of cadmium toxicity on growth and elemental composition of marine phytoplankton. J. Phycol. **35**: 293–302. doi:10.1046/j.1529-8817.1999.3520293.x

Planquette, H. and R. M. Sherrell. 2012. Sampling for particulate trace metal determination using water sampling bottles: methodology and comparison to in situ pumps. Limnol. Oceanogr. Methods **10**: 367–388. doi:10.4319/lom.2012.10.367

Planquette, H., R. M. Sherrell, S. Stammerjohn, and M. P. Field. 2013. Particulate iron delivery to the water column

of the Amundsen Sea, Antarctica. Mar. Chem. **153**: 15–30. doi:10.1016/j.marchem.2013.04.006

Redfield, A. C. 1958. The biological control of chemical factors in the environment. Am. Sci. **46**: 205–221.

Rodriguez, I. B., and T.-Y. Ho. 2015. Influence of Co and $B_{12}$ on the growth and nitrogen fixation of Trichodesmium. Front. Microbiol. **6**: 623. doi:10.3389/fmicb.2015.00623

Saito, M. A., J. W. Moffett, S. W. Chisholm, and J. B. Waterbury. 2002. Cobalt limitation and uptake in *Prochlorococcus*. Limnol. Oceanogr. **47**: 1629–1636. doi:10.4319/lo.2002.47.6.1629

Sherrell, R. M., and E. A. Boyle. 1992. The trace metal composition of suspended particles in the oceanic water column near Bermuda. Earth Planet. Sci. Lett. **111**: 155–174. doi:10.1016/0012-821X(92)90176-V

Sunda, W. G. 2012. Feedback interactions between trace metal nutrients and phytoplankton in the ocean. Front. Microbiol. **3**: 204. doi:10.3389/fmicb.2012.00204

Sunda, W. G., and S. A. Huntsman. 1995. Cobalt and zinc interreplacement in marine phytoplankton: Biological and geochemical implications. Limnol. Oceanogr. **40**: 1404–1417. doi:10.4319/lo.1995.40.8.1404

Sunda, W. G., and S. A. Hunstman. 2000. Effect of Zn, Mn, and Fe on Cd accumulation in phytoplankton: Implications for oceanic Cd cycling. Limnol. Oceanogr. **45**: 1501–1516. doi:10.4319/lo.2000.45.7.1501

Tebo, B. M., J. R. Bargar, B. G. Clement, G. J. Dick, K. J. Murray, D. Parker, R. Verity, and S. M. Webb. 2004. Biogenic manganese oxides: Properties and mechanisms of formation. Ann. Rev. Earth Planet. Sci. **32**: 287–328. doi:10.1146/annurev.earth.32.101802.120213

Tovar-Sanchez, A., S. Sañudo-Wilhelmy, A. B. Kustka, S. Agustí, J. Dachs, D. A. Hutchins, D. G. Capone, and C. M. Duarte. 2006. Impact of dust deposition and river discharges on trace metal composition of Trichodesmium spp. in the tropical and subtropical North Atlantic Ocean. Limnol. Oceanogr. **51**: 1755–1761. doi:10.4319/lo.2006.51.4.1755

Twining, B. S., S. B. Baines, and N. S. Fisher. 2004. Element stoichiometries of individual plankton cells collected during the Southern Ocean Iron Experiment (SOFeX). Limnol. Oceanogr. **49**: 2115–2128. doi:10.4319/lo.2004.49.6.2115

Twining, B. S., S. B. Baines, J. B. Bozard, S. Vogt, E. A. Walker, and D. M. Nelson. 2011. Metal quotas of plankton in the equatorial Pacific Ocean. Deep-Sea Res. Part II Top. Stud. Oceanogr. **58**: 325–341. doi:10.1016/j.dsr2.2010.08.018

Twining, B. S., S. Rauschenberg, and P. L. Morton. 2015*a*. Comparison of particulate trace element concentrations in the North Atlantic Ocean as determined with discrete bottle sampling and in situ pumping. Deep-Sea Res. Part II Top. Stud. Oceanogr. **116**: 273–282. doi:10.1016/j.dsr2.2014.11.005, 2015

Twining, B. S., S. Rauschenberg, P. L. Morton, and S. Vogt. 2015*b*. Metal contents of phytoplankton and labile particulate material in the North Atlantic Ocean. Prog. Oceanogr. **137**: 261–283. doi:10.1016/j.pocean.2015.07.001

Wen, L.-S., W.-H. Li, and G.-Z. Zhuang. 2005. Multiple layer filtering and collecting device. Taiwan Patent No. M275880.

Yang, H.-H. 2009. Phytoplankton community structure in the Northern South China Sea and West Philippine Sea. Master thesis. National Taiwan Normal Univ.

Zhuang, G., R. A. Duce, and D. R. Kester. 1990. The dissolution of atmospheric iron in surface seawater of the open ocean. J. Geophys. Res. **95**: 16207–16216. doi:10.1029/JC095iC09p16207

## Acknowledgments

We thank James Moffett and two anonymous reviewers for their invaluable comments which have significantly improved the quality of our manuscript. We thank the technical support of the personnel of *R/V Ocean Research V* and *I*, and TORI (Taiwan Ocean Research Institute). We thank Bo-Shian Wang, Chih-Ping Lee, Chia-Te Chien, and Der-Chuen Lee for their technical support on sampling and analysis. This research was financially supported by Taiwan Ministry of Science and Technology grants number 104-2811-M-001-069 and Career Development Award from Academia Sinica.

## Conflict of Interest

None declared.

*Submitted 25 March 2016*
*Revised 18 August 2016; 07 December 2016; 13 February 2017; 07 March 2017*
*Accepted 09 March 2017*

*Associate editor: James Moffett*